FLOW CASCADE ANALYSIS EMPLOYING HESS & SMITH MODIFIED PANEL METHOD AND A CDF CODE

Ramiro Gustavo Ramirez Camacho
Instituto Tecnológico de Aeronáutica- ITA
rgramirez65@hotmail.com

Nelson Manzanares Filho
Universidade Federal de Itajubá-UNIFEI
Nelson@efei.br

João Roberto Barbosa
Instituto Tecnológico de Aeronáutica- ITA
Barbosa@ita.br

Abstract*. Design of turbomachinery cascades requires the definition of some basic parameters, like the flow turning angle and the blade lift coefficient, which must be high to guarantee the high pressure rise, without compromising efficiency and withstanding high aerodynamic loadings typical of near-stall. Axial flow turbomachines usually operate at nominal conditions with significant areas of boundary layer separation, what has been observed by some researchers (Lieblein (1959) and Schlichting (1959)), and has been confirmed both theoretical, by boundary layer analysis, and experimentally, by rig-testing of cascades and axial compressors. This work shows two numerical methods that can be used to calculate flow in cascades: a modification of the Hess & Smith's panels technique and a commercial CFD code. The regions of boundary layer separation are analysed and pressure distributions calculated by these two models are compared with experimental dada for the sake of models validation.*

Keywords*: cascades, boundary layer, turbomachinery, CFD, model turbulence.*

1. Introduction

CFD has gone a long way since the early development years of the 1960' s and is today indispensable part of any design and development phase in all sectors of industry and in particular in the area of the internal channel in turbomachinery flow.

Considerable progress has been achieved on the algorithmic side and the computer hardware performance has increased by a significant factor, in terms of both speed and memory. Over the last 30 years computing power has increased by more than a factor of 10^6, while gains in algorithmic performance can be estimated as close to 10^3. As a result, full Navier Stokes codes, with 3D turbulent model, has been applied in up to 20 blade rows and many millions of points (Hirsch et al 2003)

Another important aspect is to define the turbulence model appropriately. The influence of specific turbulence model formulation on turbomachinery applications differs substantially for different types of machines. However, almost all machine types encountered situations where the formulation and proper application of the turbulence model was a key factor in the accurate prediction of the machine characteristic.

As can be observed, full Navier Stokes flow solvers are actually more utilized because they represent physical problems in a more accurate way. In the other hand, it is necessary to employ very powerful computers with very fast execution time to obtain results with high accuracy and reduced time.

In contrast, some other works, like the panels methods based on distribution of singularities, have been applied for calculation of potential fluid field both in isolated and cascaded airfoils. In these methods the viscous effects are quantified through transpiration, with the normal velocities obtained from developed boundary layer (Lighthill, 1958). They are also known as "inviscid/viscous interaction" methods. These techniques offer satisfactory results, especially in situations where boundary layer separation has not yet been detected in the proximity of the trailing edge (Bizarro and Girardi, 1998). In that work a transpiration velocities distribution on body surface, determined through boundary layer integral solution calculation, was used for viscous calculations. In this work another formulation of the technique of the panels is presented, incorporating two modifications: the first, in the boundary conditions to simulate the viscous effect; the second, in the separation of the boundary layer.

Works based on coupled inviscid-viscous interaction, where the potential model is determined through singularity distributions around airfoils and integral methods of boundary layer to determine the viscous effect, have the advantage of less computational effort compared to full Navier-Stokes solution models, as shown previously. The potential model based on boundary elements such as the panel's technique, is more appropriate for inviscid flow calculation because it does not require iteration and can be considered as fully accurate at each stage and consequently it requires less computational effort compared to the other methods.

Considering these aspects, the use of alternative methods with low computational cost, may be attractive in the turbomachinery preliminary design. Ramirez and Manzanares (2000) have proposed a model for the simulation of boundary layer separation in cascades of turbomachinery based on the Hess and Smith (1967) panel technique. The classical impenetrability condition on the blade surface was modified by flow injection in the area of separation, according to the empirical procedure by Hayashi & Endo (1977). In the situation there is no boundary layer separation, transpiration velocities are introduced according to the Lighthill, (1958) formulation. Results for pressure distributions, flow turning angles and aerodynamic coefficients have been compared to experimental data from NACA-65 airfoil cascades.

In the present work are analysed and compared the pressure distribution in cascades of turbomachinery, obtained from two methods: the flow injection and transpiration technique (panel method) and a CFD technique using the full Navier Stokes equations and turbulence modelling. The software FLUENT (2003) was used for the calculations. Results for the pressure distribution on the airfoil are compared with experimental data.

In the design of turbomachinery cascades it is often necessary to define some basic parameters such as the flow turning angle and the blade lift coefficient. These parameters must be high enough to guarantee the highest pressure rise through the machine without compromising its efficiency with aerodynamic loadings typical of stall. The result is that axial flow turbomachines usually operate at nominal conditions with significant areas of boundary layer separation. This fact has been observed by some researchers such as Lieblein (1959), and has been confirmed theoretically by boundary layer analysis and experimentally in tunnels of cascades and axial compressor rig. Therefore situations of flow separation must be necessarily considered in the preliminary design. Bearing this in mind, it's important to give attention to the boundary layer separation, with which usually the turbomachines run, what influences lift and drag.

2. Formulation of the Equations for the Flow in Linear Cascades

Linear cascades are plane cascades derived from the axial flow machinery cylindrical cascades. Fig. (1) shows a scheme of an infinite linear grid in the complex plane $z = x + \hat{i}y$, where x is the axial axis and $\hat{i}$ is the imaginary unity $\sqrt{-1}$.

The cascade is composed of identical profiles equally spaced with pitch t, chord length l and stager angle β, angle between blade chord and axial direction and solidity $\lambda = l/$.

The study of the relative velocity field $\vec{W}$ in the cascade is desired, as well as in the region outside the profiles. The assumptions of potential, incompressible, steady and bi-dimensional flow is considered here. The flow parameters are represented by the flow angles in the inlet and outlet, β_1 and β_2 respectively, the deflection angle of the flow in the cascade, $\Delta\beta = (\beta_1 - \beta_2)$; and by flow velocities in the inlet and outlet, $\vec{W}_1$ .and $\vec{W}_2$, respectively.

The velocity of the undisturbed flow is given by the average of the vector velocities in the inlet and the outlet: $\vec{W}_\infty = (\vec{W}_1 + \vec{W}_2)/2$. The circulation on the velocity field around the profile is defined by $\Gamma_P = \oint W_{\tan} ds$, where $W_{\tan}$ is the outer tangential velocity at the profile boundary. Figure 1 shows the geometry of a linear cascade and its velocities diagram.

3. Hess and Smith Panel Method for Cascades

Details of the basic formulation of the Hess and Smith (1967) panel method are detailed depicted by Petrucci (1998). The airfoil is approximated by an inscribed polygon selected to give a reasonable representation of the airfoil contour. The segments of polygons are denominated panels, usually concentrating a larger quantity of these segments in the region of the leading and trailing edges. Uniform distributions of sources and vortex are used; the intensities of sources are the variables and the intensities of vortex are specified as a sinusoidal function that becomes zero at the trailing edge and reaches the maximum value γ_{max} at the leading edge.

It is important to notice that the numerical technique of Hess and Smith (1967) was first implemented to study the flow in isolated profiles for flight aerodynamics. In that technique the angle of attack, α_∞, is measured relative to the profile chord, and the velocity $\vec{W}_\infty$ is used for the calculation of the distribution of singularities. For cascades of profiles as in turbomachinery rotors, the inlet velocity, W_1, and the inlet angle, β_1, measured relative to the axial direction (Emery et al, 1957) are usually fixed. To obtain the angle β_1, in the first situation, different values of α_∞ must be tested iteratively, until a circulation is obtained around the airfoil compatible with velocities diagram (Fig.1). This process increases significantly the time of computation, mainly when it is intended to make viscous/non-viscous interactions. Consequently it is convenient to reformulate the method of Hess and Smith to give directly the cascade inlet angle and to perform the potential calculation straight, without iterations. Given that these considerations can be obtained on integral form, the component of the normal velocity W_n and tangential velocity W_t to the profile surface are then isolated:

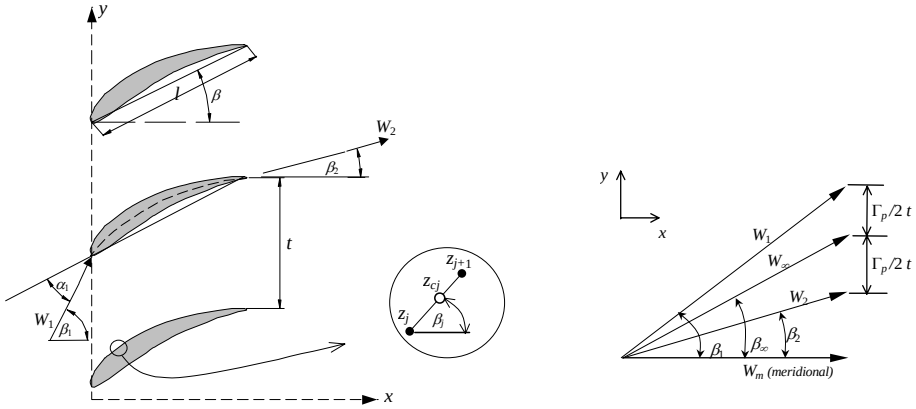

Figure 1. Linear cascade and velocity diagram.

$$W_{t_i} = \mathcal{Re}\left\{\sum_{j=1}^{N}\frac{\sigma_j e^{-\hat{i}\beta_j}}{2\pi}\log(K)e^{\hat{i}\beta_i} + +\gamma_{\max}\hat{i}\left(\sum_{j=1}^{N}\frac{e^{\hat{i}\beta_j}}{2\pi}\log(K)\cdot e^{\hat{i}\beta_i}\cdot F_i + (P)e^{\hat{i}\beta_i}\right) + W_1 e^{-\hat{i}\beta_1}\cdot e^{\hat{i}\beta_i}\right\}, \tag{1}$$

$$W_{n_i} = -\mathcal{Im}\left\{\sum_{j=1}^{N}\frac{\sigma_j e^{-\hat{i}\beta_j}}{2\pi}\log(K)e^{\hat{i}\beta_i} + \gamma_{\max}\hat{i}\left(\sum_{j=1}^{N}\frac{e^{\hat{i}\beta_j}}{2\pi}\log(K)\cdot e^{\hat{i}\beta_i}\cdot F_i + (P)e^{\hat{i}\beta_i}\right) + W_1 e^{-\hat{i}\beta_1}e^{\hat{i}\beta_i}\right\}, \tag{2}$$

where K is the argument of the logarithmic function:

$$K_{(z_{c_i},z_j)} = \left[\frac{\sinh(z_{c_i}-z_j)/t}{\sinh(z_{c_i}-z_{j+1})/t}\right]; \qquad P = \frac{\sum_{j=1}^{N}F_i\Delta s_i}{2\cdot t} \qquad F(s) = \frac{1}{2}\left[1+\sin\left[\pi\left(\frac{2\cdot s}{s_l}-\frac{1}{2}\right)\right]\right]. \tag{3abc}$$

Details of the calculation of the circulation around the blade are given by Ramirez and Manzanares (2001). The equations (1) and (2) can be rewritten in matrix form:

$$\{W_t\} = [B]\{\sigma\} + \gamma_{\max}\{D\} + \{W^1_{tan}\}, \tag{4}$$

$$\{W_n\} = [A]\{\sigma\} + \gamma_{\max}\{C\} + \{W^1_{nor}\}. \tag{5}$$

The brackets {} represent column vectors Nx1 and the square brackets [ ] square matrices $N \times N$. [A] and [B] are the matrices of the normal and tangential influence coefficients, respectively, that depend only on the geometry of the airfoil, the blade pitch, the stagger angle, and the number of panels; {D} and {C} represent the vectors of the normal and tangential influence of vortex; $\{W^1_{tan}\}$ and $\{W^1_{nor}\}$ are the vectors of the normal and tangential components in the cascade inlet; $\{W_n\}$ is the vector of the normal velocity imposed at the profile boundary.

According to the method of Hess and Smith for the potential flow around the bodies, the variables γ_{max} (vortex) and σ (source) from Eqs. (4) and (5) are determined by the simultaneous application of the two conditions. The first is the boundary condition of the impenetrability that requires a null normal velocity over the body surface: $W_n = 0$; the second is the Kutta Condition that requires a flow that doesn't turn around the trailing edge. One way to impose this condition is to requires the tangential velocities on the control points over panels of the trailing edge to be the same, but in the opposite direction, that is, $W_{tn} = -W_{t1}$. The following chapter will treat the breakaway and the modifications of normal velocities of transpiration in the boundary condition as well as the Kutta's Condition.

3.1 Separated Wake Simulation

The boundary condition of the normal velocity W_n (Eq. 5) can be modified in order to simulate the wake breakaway through the fictitious flow injection. Hayashi and Endo (1977) obtained a semi-empirical relationship that

quantifies the flow to be injected into the portion of separation flow. They use the tangential direction of the breakaway velocity W_s on the point s_u (upper) and s_l (lower), defined by the angles β_u and β_l respectively, as shown in Fig.2a. The direction of the flow is given by the angle β^* in a random point on the profile surface between the points s_u and s_l, and it is admitted that the normal component of the velocity vary in a linear way with the distance s along the surface.

Based on the experimental data, Hayashi and Endo (1977) defined a semi-empirical correlation was obtained between the non-dimensional flow intensity and the angles β_u and β_l, applicable to different kinds of aerodynamic bodies, Eq (6).

$$Q_E / l_{sp} W_s = 0.25 + 0.55\cos\left(\frac{\beta_u + \beta_l}{2}\right) + 1.70\, sen\left(\frac{\beta_u - \beta_l}{2}\right) - 1.26\cos\left(\frac{\beta_u + \beta_l}{2}\right) sen\left(\frac{\beta_u - \beta_l}{2}\right) \tag{6}$$

where Q_E is the flow to be injected, W_s is the velocity in the breakaway point and l_{sp}, β_u, β_l, are the profile geometric parameters as shown in Fig. 2. The correlation was established in order to produce an approximate constant pressure in the separated wake.

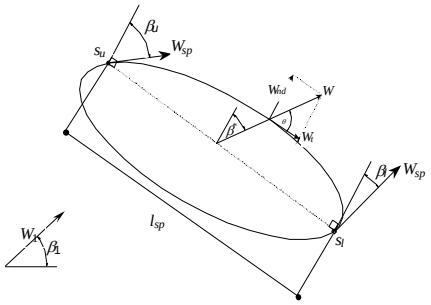

Figure 2. Definition of the normal velocity component, W_{nd}..

3.2 Effect of Attached Boundary Layer

The effect of the attached boundary layer will be treated by the technique of "*transpiration*" that consists of fluid injection in the external flow based on the boundary layer displacement thickness. This technique was proposed originally by Lighthill (1958). Represented by the following expression:

$$W_{nt} = \frac{d}{ds}(W_t \delta^*) \,. \tag{7}$$

In the Eq.(9) W_t is the outlet tangential velocity distribution in the boundary layer, calculated by the potential model, $\delta^*(s)$ is the distribution of the displacement thickness obtained from the boundary layer calculation and s is the natural coordinate around the profile.

To determine the displacement thickness distribution δ^*, boundary layer momentum thickness θ, form factor $H = \delta^*/\theta$, superficial friction coefficient c_f and point of separation, the von Kármán equation of *momentum*, is solved numerically, given a known velocity distribution (which means to specify the pressure gradient). To solve this equation, the following methods and criterions are established: integral method of Thwaites for the area of laminar boundary layer; Michel's criterion for the transition between laminar and turbulent; and Head for the turbulent, boundary layer. The turbulent separation is defined by the form factor H = 2,4. The computational code for the calculation of the boundary layer was obtained from the work of Cebeci & Bradshaw (1977).

It is important to notice that the boundary layer code used in this work doesn't allow modeling the possible formation of displacement bubbles on the surface of the aerodynamic profile. This irregularity occurs when, at adverse pressure gradient, the *laminar* boundary layer is separated and subsequently, reattached in a turbulent condition. For example, it is possible to detect the circulation bubbles in the experimental curves of pressure coefficient in the NACA 65 profile cascades, operating with an intermediate Reynolds number around 10^5 (Emery et al, 1957). The clue is to identify the tendency of the formation of a constant pressure platform after the minimum pressure point on the profile suction side (that normally limits the end of the stable laminar area). The well successful modeling of the separated bubble, remains as an opened theme, requiring further development, beyond the scope of this work.

3.3 Extended Hess and Smith Method for Aerodynamic Profiles With and Without Separation

The proposed extension my be used at any portion of the attached boundary layer considering the corresponding viscous effects quantified through the transpiration technique. In the separation area the extension will have value only

for profile suction side breakaway situations. In this area the theoretical injection flow Q_T is given by separated normal velocities (W_{nd}) and by the length ΔS of the outline distance with separation, assuming that the velocity W_{nd} raises linearly from zero at the separation point:

$$Q_T = \sum_{i=p_s}^{N} W_{nd_i} \Delta S_i / 2 , \tag{8}$$

where: p_s is the index that represents the separation point (random beginning), ΔS is the length along the profile surface in the breakaway area, and N the number of panels.

Connecting appropriately Eqs. (8) and (6) and incorporating the transpiration velocities, one has:

$$\{W_n\} = \frac{2 f(\beta_u, \beta_l) W_s}{l_{sep}} \{S\} + \{W_{nt}\} \tag{9}$$

$$\{W_n\} = \{K\} W_s + \{W_{nt}\} ; \qquad \{K\} = \frac{2 f(\beta_u, \beta_l)}{l_{sep}} \{S\} , \tag{10ab}$$

where, W_s is the separation velocity and {S} is the local coordinate vector of the separation area from the separation point. In Eq. (10a) the first term of the right represents the normal injection velocity vector that is a function of the separation velocity W_s and of the geometrical parameters: β_u, β_l, I_{sep} and S_i. The second term, the transpiration velocity of the attached boundary layer, is the vector of normal velocity around the aerodynamical body W_n. It is possible to substitute the outline assumption of W_n (Eq. 9) in Eq. (5), resulting in the following matrix equations:

$$\{K\} W_s + \{W_{nt}\} = [A]\{\sigma\} + \gamma_{\max} \{C\} + \{W^1_{nor}\}, \tag{11}$$

$$\{W_t\} = [B]\{\sigma\} + \gamma_{\max} \{D\} + \{W^1_{tan}\}. \tag{12}$$

Substituting the source intensity σ from Eq. (11) in Eq. (12):

$$\{W_t\} = \left(-[B][A]^{-1} \left(\{W^1_{nor}\} + \{W_{nt}\} \right) + \{W^1_{tan}\} + \gamma_{\max} \left(-[B][A]^{-1} \{C\} + \{D\} \right) + W_s [B][A]^{-1} \{K\} \right) \tag{13}$$

Making all the matrix operations on the Eq.(13), it results:

$$\{W_t\} = \{VINF\} + \gamma_{\max} \{VGAMA\} + W_s \{VNOR\} \tag{14}$$

Note that in Eq. (13), vortex intensity $\gamma_{\max}$ and the velocity W_s are unknown which may be calculated by a change in the Kutta's condition, that is, the velocity at the separation point W_s will be the same as the velocity at the trailing edge in the lower side; $W_s = W_{ps} = -W_1$. From Eq. (14), it can be obtained the system of two equations with two variables W_s and $\gamma_{\max}$, where the subscript 1 refers to the first panel of the trailing edge on the lower side and p_s to the panel where the separation point is fixed in first instance.

The value of the pressure coefficient, C_p, is calculated taking in to count the component of the normal and tangential velocities:

$$C_{p_1} = 1 - \left(\frac{W_{\tan}}{W_1} \right)^2 - \left(\frac{W_n}{W_1} \right)^2 \tag{15}$$

4. Turbulence Model Formulation Consideration.

Turbulence modelling has been an issue for CFD simulations of turbomachines over many decades. The influence of specific turbulence model formulations on turbomachinery applications differs substantially for different types of machines. However, almost all machines types have encountered situations, where the formulation and proper application of the turbulence model was a key factor in the accurate prediction of the flow in the turbomachinery.

Some of the most well known rules for turbulence model selection for turbomachinery flows are. a) For flow with adverse pressure gradient and pressure-induced separation do not use the κ-ε model. More advanced models, like the Spalart-Allmaras model, provide more realistic answer. The κ-ε model do not predict the separation point correctly b) For flows with heat transfer and flow reattachment, attention must be given to possible large overshoot with some low-

Reynolds number κ-ε models. All κ-ε, or modern κ-ε models like the v2f model, are more appropriate. For standard k-ε models use limiters, like the Yap correction. c) For massively separated flows, consider the use of DES methods (Menter, 2003).

The Reynolds-averaged Navier-Stokes (RANS) equations represent transport equations for the mean flow quantities only, with all the scales of the turbulence being modelled. The approach of permitting a solution for the mean flow variables greatly reduces the computational effort. If the mean flow is steady, the governing equations will not contain time derivatives and a steady-state solution can be obtained economically. A computational advantage is seen even in transient situations, since the time step will be determined by the global unsteadiness in the mean flow rather than by the turbulence. The Reynolds averaged approach is generally adopted for practical engineering calculations, and uses models such as Spalart-Allmaras, κ-ε and its variants, and the RSM.

In Reynolds averaging, the solution variables in the instantaneous (exact) Navier-Stokes equations are decomposed into the mean (ensemble-averaged or time-averaged) and fluctuating components. For the velocity components: $u_i = \bar{u}_i + u_i'$, where $\bar{u}_i$ and u_i' are the mean and fluctuating velocity components (i = 1; 2; 3). For pressure and other scalar quantities; $\phi = \bar{\phi} + \phi'$, where ϕ denotes a scalar such as pressure, energy, or species concentration. Substituting expressions of this form for the flow variables into the instantaneous continuity and momentum equations:

$$\frac{\partial}{\partial x_i}(\rho u_i) = 0\,, \tag{17}$$

$$\frac{\partial}{\partial x_i}(\rho u_i u_j) = -\frac{\partial p}{\partial x_i} + \frac{\partial}{\partial x_i}\left[\mu\left(\frac{\partial u_i}{\partial x_i} + \frac{\partial u_j}{\partial x_i} - \frac{2}{3}\delta_{ij}\frac{\partial u_l}{\partial x_l}\right)\right] + \frac{\partial}{\partial}(-\rho\overline{u_i'}\ \overline{u_j'}\ )\,. \tag{18}$$

Equations (17) and (18) are called Reynolds-averaged Navier-Stokes (RANS) equations. They have the same general form as the instantaneous Navier-Stokes equations, with the velocities and other solution variables now representing ensemble-averaged values. Additional terms now appear that represent the effect of turbulence. These Reynolds stresses, must be modelled in order to close Equation (18), (Wilcox 1994).

4.1 Transport Equation for the Spalart-Allmaras Model:

The Spalart-Allmaras (1992) model was designed specially for aerospace applications involving wall-bounded flows and has been shown to give good results for boundary layers subjected to adverse pressure gradients. It is also gaining popularity for turbomachinery applications. In its original form, the Spalart-Allmaras model is effectively a low-Reynolds-number model, requiring the viscous-affected region of the boundary layer to be properly resolved. In the FLUENT software, however, the Spalart-Allmaras model has been implemented to use wall functions when the mesh resolution is not sufficiently fine.

The transported variable in the Spalart-Allmaras model, $\tilde{\nu}$, is identical to the turbulent kinematic viscosity, except in the near-wall (viscous-affected) region. The transport equation for $\tilde{\nu}$ is:

$$\frac{\partial}{\partial x_i}(\rho\tilde{\nu}u_i) = G_\nu + \frac{1}{\sigma_\nu}\left[\frac{\partial}{\partial x_i}\left\{(\mu + \rho\tilde{\nu})\frac{\partial\tilde{\nu}}{\partial x_i}\right\} + C_{b2}\rho\left(\frac{\partial\tilde{\nu}}{\partial x_i}\right)^2\right] - Y_\nu + S_{\tilde{\nu}} \tag{19}$$

where G_ν is the production of turbulent viscosity and Y_ν is the destruction of turbulent viscosity that occurs in the near-wall region due to wall blocking and viscous damping. $\sigma_{\tilde{\nu}}$ and C_{b2} are constants and ν is the molecular kinematic viscosity. $S_{\tilde{\nu}}$ is a user-defined source term.

5. Pressures Distribution: Examples of Application.

The results obtained through the technique of flow injection and transpiration, using the panel method and the numerical model applying finite volumes for a cascade of NACA 65 airfoils were validated according to the experimental results from Emery et al (1957).

Figure 3 shows the results of the pressure distribution for different angles of attack (α_1), keeping the cascade solidity (λ=0.5) constant. Figure 3a presents the potential, flow injection-transpiration models and CFD-Fluent results and shows good agreement for an angle of attack (α_1) of 21,7° when compared with experimental dada.

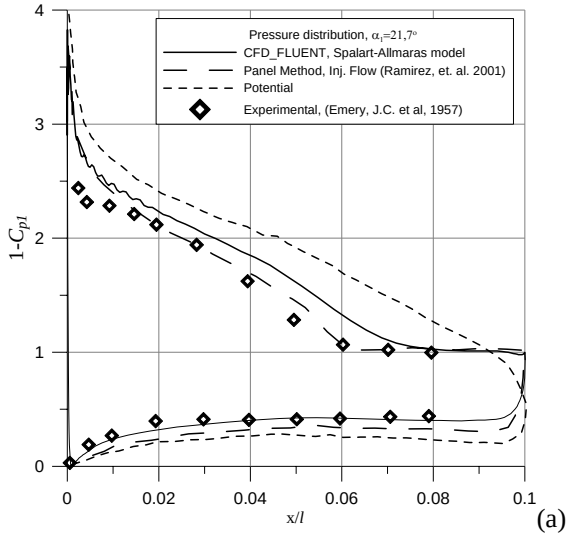

(a)

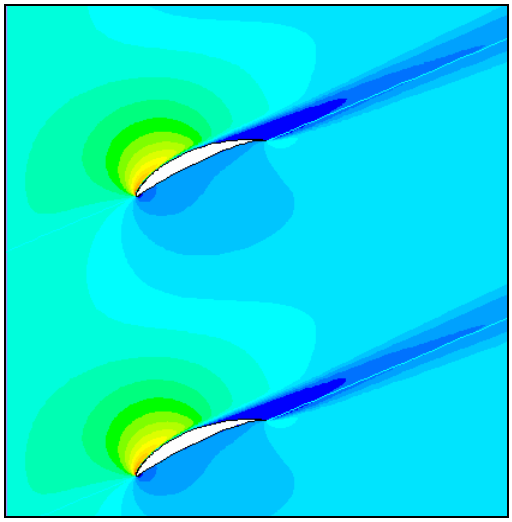

(b)

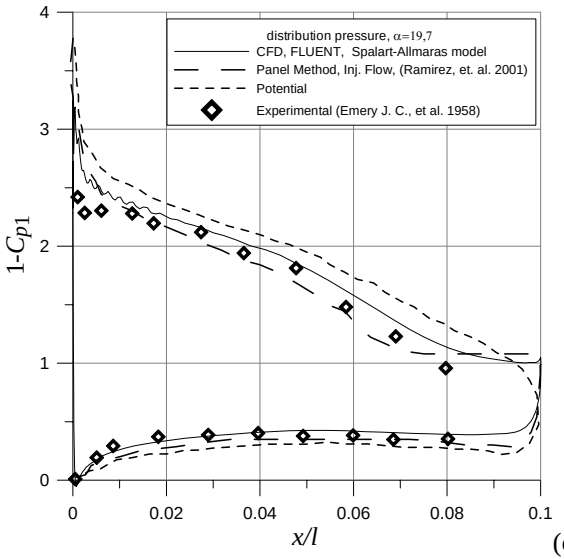

(c)

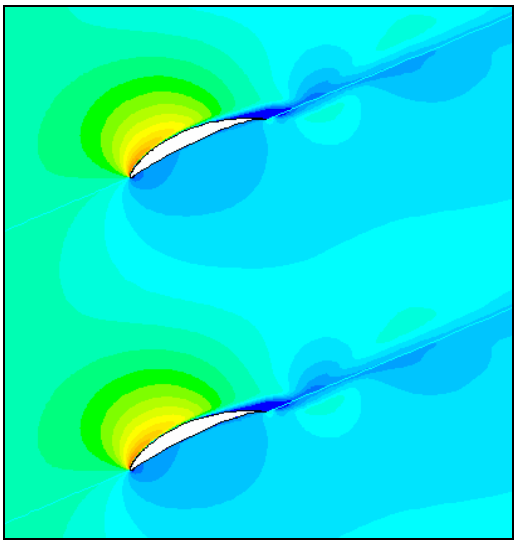

(d)

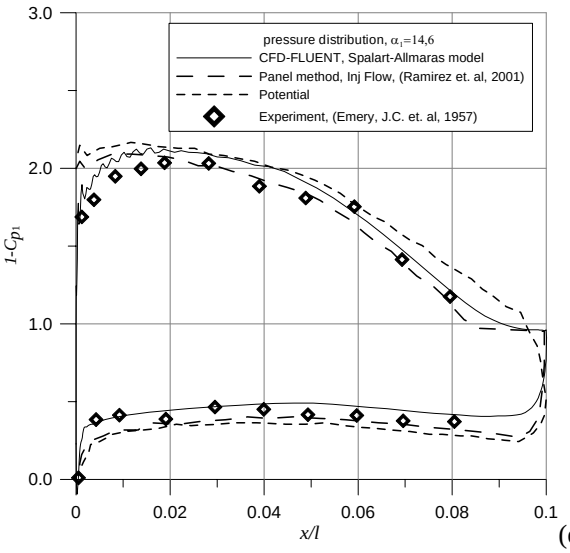

(e)

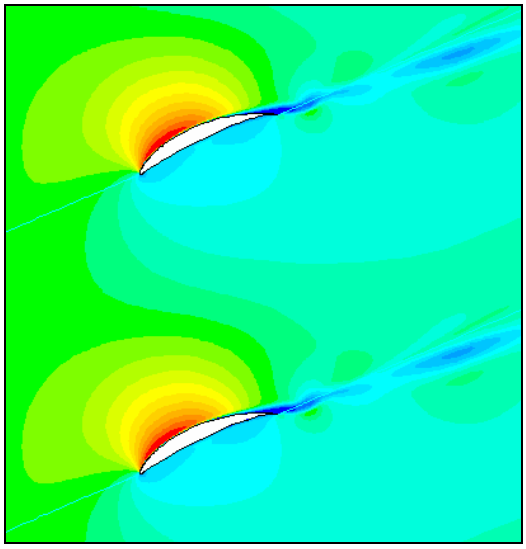

(f)

Figura 3. a) Pressure distribution, NACA65-(18)10, λ=0.5, Reynolds 2.45×10^5, $\beta = 23.3^o$, (Fig 1)
b) Contours pressure dynamic, Viscous model Spalart Allmaras

It is worth noting that the interaction of viscous and inviscid models is more precise in determining the flow separation point where, from this point on, the constant pressure is taking account. Figure 3b describes the dynamic pressure curves, where it can be seen the wake conformation and the regions where there pressure gradients are the greatest.

Fig 3c shows a good agreement of the CFD calculations, when the Spalart-Allmaras turbulence model is employed. It is noticed that there are not any experimental data in the trailing edge region. This is probably due to the difficulty of installing measurement devices that generate static pressure values, due to the short airfoil chord (5 cm). It may be concluded that the information obtained from the numerical models are useful for the analyses at the early stage of the project: It can be confirmed from the static pressure diagrams (Cp) and from the total pressure outlines (Figs 3b, 3d and 3f).

Finally, an operating point close to the design point (Ramirez 2001), where small separation prevail around 15% of the chord length is presented in Fig 3(e) and (f).

6. Conclusions

The Hess & Smith (1976) modified method to simulate the flow in cascades, employing the flow injection technique and transpiration velocities, together with CFD code, using Spalart-Allmaras turbulence model, produced satisfactory results for pressure distributions. The results showed the strong influence of the flow injection, especially near the stall region.

Turbulence modelling will certainly continue to play a major role in the simulation of turbomachinery flows. Although the Spalart-Allmaras model used in this work gave good results, it is necessary to adjust the wall law functions properly, in order to obtain more realistic results for the friction, drag and loss coefficients, as well as the deflexion angle.

7. Acknowledgments

The author would like to thank for technical support given to this work investigation by the Fundaçao de Amaparo à Pesquisa do Estado de São Paulo, FAPESP and Marco Aurelio Santin MSc. student in the construction of the mesh.

8. References:

Cebeci, T., Bradshaw, P., 1977, “Momentum Transfer in Boundary Layers”, McGraw-Hill/Hemisphere, Washington, D.C.

Emery, J.C., Herrig, L.J., Erwin, J. R., Felix, R., 1957, “Systematic Two- Dimensional Cascade Tests of Naca 65-Series Compressor Blades at Low Speeds”, NACA TN 1368, pp-23

Fluent 6.1 User's Guide, February 2003

Hayashi, M., Endo, E., 1977, “Performance Calculation for Multi-Element Airfoil Sections with Separation”, Trans. Japan Soc. Aero. Space Sci.,Vol 20, Nro 49.

Hess, J.L., Smith, A.M.O., 1967, “Calculation of potential Flow About Arbitrary Bodies”, Progress in Aeronautical Sciences, Pergamon Press, vol. 8, pp. 1-138.

Hirsch, C., Demeulenaere, A., 2003 “State of the Art in the Industrial CFD for Turbomachinery Flows” QNET-CFD Network Newsletter, Volume 2, No. 3.

Lieblein S., 1959, “Loss and Stall Analysis of Compressor Cascades”, Journal of Basic Engineering, pp 387- 400.

Lighthill, M.J., 1958, “On displacement Thickness”, J.F1 Mech., 4, pp.383

Meter F. R. , 2003, “Turbulence Modelling for Turbomachinery”, QNET-CFD Network Newsletter, Vol. 2, No. 3

Petrucci, R.D., 1998, “Problema Inverso do Escoamento em Torno de Perfis Aerodinâmicos Isolados e em Grades de Turbomáquinas”, Tese de Mestrado, EFEI, Itajubá – MG, Brasil.

Ramirez R.G.C., 2001, “Análise do Escoamento em Grades de Turbomáquinas Axiais Incluindo o Efeito de Separação da Camada Limite” (In Portuguese), Tese Doutorado, Escola Federal de Engenharia de Itajubá, M.G

Ramirez, R.G., Manzanres, N.F., 2000, “Extensão do Método de Hess & Smith para Cálculo do Escoamento em Grades com Separação”, Anais-CD, VIII Congresso Brasileiro de Ciências Térmicas, ENCIT 2000, Porto Alegre - Brasil.

Spalart.,P.R., Allmaras, S.R., 1992, “ A One-Equation Turbulence Model for Aerodynamics Flows”, AIAA Paper 92-0439.

Wilcox., D.C., 1994, “Turbulence Modeling for CFD”, DCW Industries, Inc, La Cañada, California.

9. Responsibility notice.

The author(s) is (are) the only responsible for the printed material included in this paper.